

COMPARING MECHANICAL AND GEOMETRICAL PROPERTIES OF LATTICE STRUCTURE FABRICATED USING ELECTRON BEAM MELTING

Sang-in. Park^a, David W. Rosen^a, and Chad E. Duty^b

^aThe G. W. Woodruff School of Mechanical Engineering, Georgia Institute of Technology,
Atlanta, GA 30332

^bOak Ridge National Laboratory, Oak Ridge, TN 37831

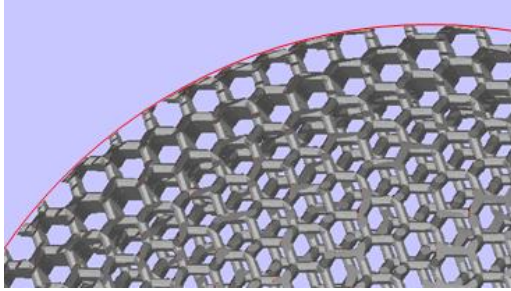
ABSTRACT

To design lattice structure, a uniform voxel based approach is widely used which divides a part into unit volumes (e.g., cubes) and maps lattice topology into those volumes. In contrast, conformal lattice structures represent a second design method for constructing lattices in which unit cells are constructed parallel to the surface to be reinforced and are deformed in a manner that enables them to conform to the surface. In this paper, the strength of lattice structures designed using these two methods (uniform voxel based and conformal) are compared based on additive manufacturing (AM) process effects. For this purpose, spheres filled with three types of lattice structure are fabricated using electron beam melting technology and tested in compression. Effects of AM processes are studied in two ways – volumetric and structural performance equivalence. Struts in lattice structures are observed through a microscope to examine volume-equivalence and tests are simulated numerically and compared to identify structural equivalence.

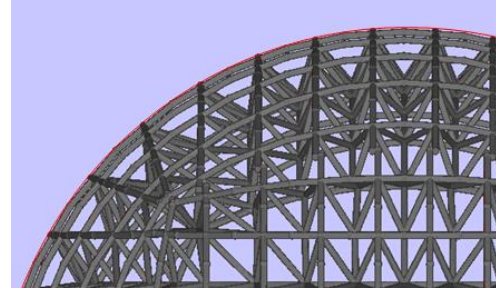
1 INTRODUCTION

Cellular materials such as foam, honeycomb, and lattice structure are used in applications due to their special mechanical properties which cannot be achieved by conventional bulk material. The use of cellular material expands the design space for mechanical properties [1]. Generally, cellular materials can be tailored for high strength to weight ratio, thermal conductivity and energy absorbance [2]. A lattice structure is one type of cellular material which is comprised of a connected network of struts. Among the cellular material, the lattice structure has a distinguished characteristic, which is lattice structures are composed of representative unit cells that define their geometries and topologies. This enables engineers to design mechanical properties of lattice structures such as elastic modulus, yield strength and fracture strength for specific applications [1, 3].

There are two approaches for designing the lattice structures – a uniform and a conformal lattice approaches [4]. In the uniform approach, the volume of a part is divided into small regular blocks and the topology of unit cell is mapped into the blocks. Lattice structures can be simply obtained through this process and struts inside lattice structures are fully connected. However, obtained lattice structures often become broken or unconnected near surfaces as Figure 1 (a).



(a) Uniform lattice approach



(b) Conformal lattice approach

Figure 1 Design approach for lattice structure

The conformal lattice structure approach is proposed to solve the problem of broken struts at part boundaries [5]. In the conformal lattice approach, conformal hexahedral meshes on the target surfaces are created and unit cells are mapped into the meshes. Since meshes from the mapping process conform to target surfaces, the struts are fully connected as shown in Figure 1 (b)

Although lattice structures generally give better properties than other cellular materials, complex geometries in lattice structures make it difficult [6, 7] or impossible to manufacture lattice structures using conventional manufacturing methods. Additive manufacturing (AM) technologies can be a solution for the problems in manufacturing lattice materials. Since AM processes deposit materials layer by a layer based on slicing information of parts, lattice structures can be easily fabricated without a consideration for tool interference. Through the past two decades, various AM processes have been used to fabricate lattice structures. The Electron Beam Melting (EBM) process is one such AM process which uses an electron beam to melt metal powder and form the shape of part cross-sections. Recently, this process has been applied to build lattice structure with Ti6Al4V metal powder [8, 9].

Fabricating lattice structure takes advantage of AM processes. However, the processes introduce shape variations which are geometrical fluctuation or errors of fabricated features compared to their designed shapes and sizes. Since the AM processes deposit material based on cross sectional layer information, fabricated parts have stair steps [10, 11]. Additional factors cause geometric deviations in the EBM process. Since metal powder is selectively melted by the electron beam, the unmelted powder near melt pools can become stuck on the part surfaces. This phenomenon makes the surfaces rough and uneven. Yang et al. reported that struts in fabricated lattice blocks show dimensional variations due to Ti6Al4V powder particles [12]. Parthasarathy et al. evaluated EBM processed lattice blocks using 3D digital reconstructions and showed variations in dimensions of the blocks [13]. Recently, List et al. studied the relationship between process parameters and geometrical and mechanical parameters [14]. Previous researches indicate that AM processes affects geometrical dimensions as well as mechanical properties of manufactured parts.

The goal of this paper is to study the effects of the EBM AM process on geometrical and mechanical properties of fabricated lattice structure. To achieve the goal, two research questions are investigated; which design method between the uniform and conformal lattice approach gives better mechanical properties? and how to quantitatively measure shape variations resulting from the additive manufacturing process? We hypothesize that conformal lattice structure will have higher fracture strength for the first question and geometrically and mechanically equivalent values of strut diameters can be used for measuring shape variations for the second question. In this paper, three tasks are conducted in order to test hypotheses. Related to the first research question, fracture strengths of meshed balls fabricated by EBM process are compared, which are designed by the two design approaches. Related to the second research question, the mass-equivalent strut diameter is determined for meshed balls based on microscopic observation and design tools and the response-equivalent strut diameter is calculated based on comparison of compression tests and numerical analysis.

2 FABRICATION OF SPECIMENS

2.1 Design of Specimens

As specimens, four kinds of meshed balls were designed by uniform and conformal approaches. Schematic procedures for designing meshed balls are shown in Figure 2. The main difference between the two approaches is the meshing process. In the uniform lattice, regular meshes fill the volumetric region of the balls and the meshed balls have unit cells mapped into these regular meshes. However, in the conformal lattice, meshes are generated on selected base surfaces and meshed balls are constructed by generating a layer of hexahedra mesh elements, then mapping the unit cell into the elements. For the uniform lattice, the commercial software package, Magics, was used. For the conformal lattice, the TrussCreator software package was used, which is a plug-in for the Siemens NX CAD system [15].

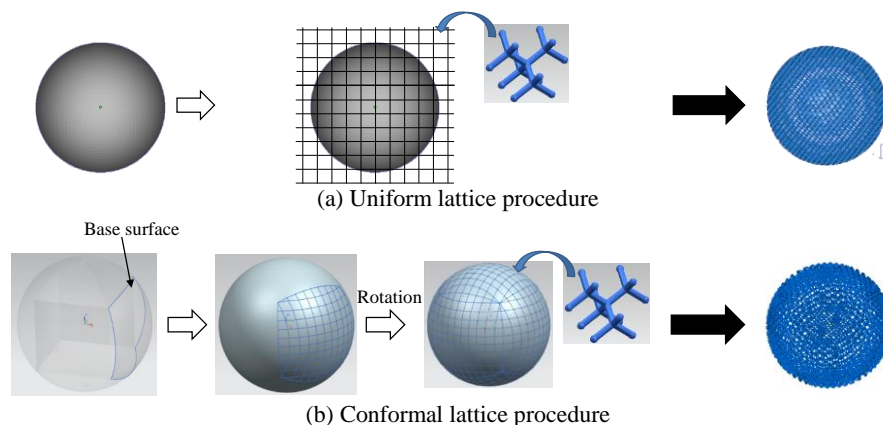


Figure 2 Schematic procedure of lattice design procedure

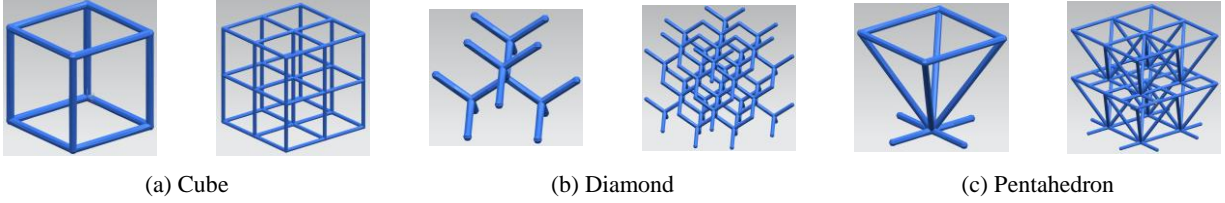
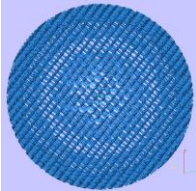
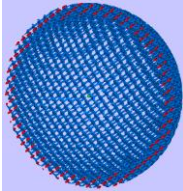
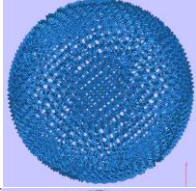
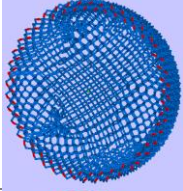
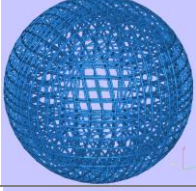
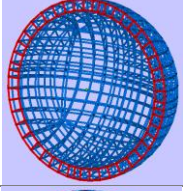
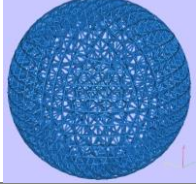
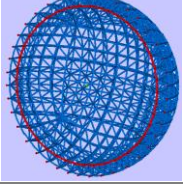


Figure 3 Unit cell type

The meshed balls are comprised of three types of unit cells, which are presented in Figure 3. Designs and specifications of the meshed balls are listed in Table 1. Design 1 is designed by the uniform lattice procedure and Designs 2, 3 and 4 are constructed by the conformal lattice procedure. Design 1 and 2 are composed of the diamond unit cell. Design 3 and design 4 are comprised of cube and pentahedron unit cells, respectively. To keep the mass of all mesh balls similar, the strut diameters in the meshed balls were not kept constant, but were adjusted. The design strut diameters of designs 1 and 2 are 0.4 mm and 0.35 mm, respectively. The design strut diameter of design 3 is 0.4 mm and 0.35 mm is used for design 4. The volume is calculated in Magics.

Table 1 Design of meshed balls

	Design		Design approach / Unit cell type	Strut Diameter (mm)	Volume (mm ³)
	Whole design	Cross section			
1			Uniform / Diamond	0.4	1210
2			Conformal / Diamond	0.35	1232
3			Conformal / Cube	0.4	1041
4			Conformal / Pentahedron	0.35	1080

It is worth noting that the conformal lattice balls have one complete layer of lattice structure, while Design 1, with uniform lattice, has one layer in most regions, but this layer is truncated, as seen in the upper left and lower right regions of the cross section view in Table 1.

2.2 Fabricated Specimens

Nine meshed balls (two of designs 1, 2, 3 and three of design 4) were built in the Arcam A2 at Oak Ridge National Laboratories using Inconel 718 metal powder. The “Net” theme was used in the Arcam 3.2 EBM control software for melting the powder. The beam current was 2.5 mA and the beam speed was 300 mm/s. The fabricated meshed balls are shown in Figure 4. The fabricated masses are compared with estimated masses using the reference density (0.00819 g/mm³) of Inconel 718 and reported in Table 2. The masses are at least 145% more than that estimated for the designed balls. The unmelted powder stuck on strut surfaces and manufacturing tolerance generated variations in the geometrical dimensions and increased the size of the struts. These lead to more mass in the meshed balls. The amount of increases is quantified in the later sections.

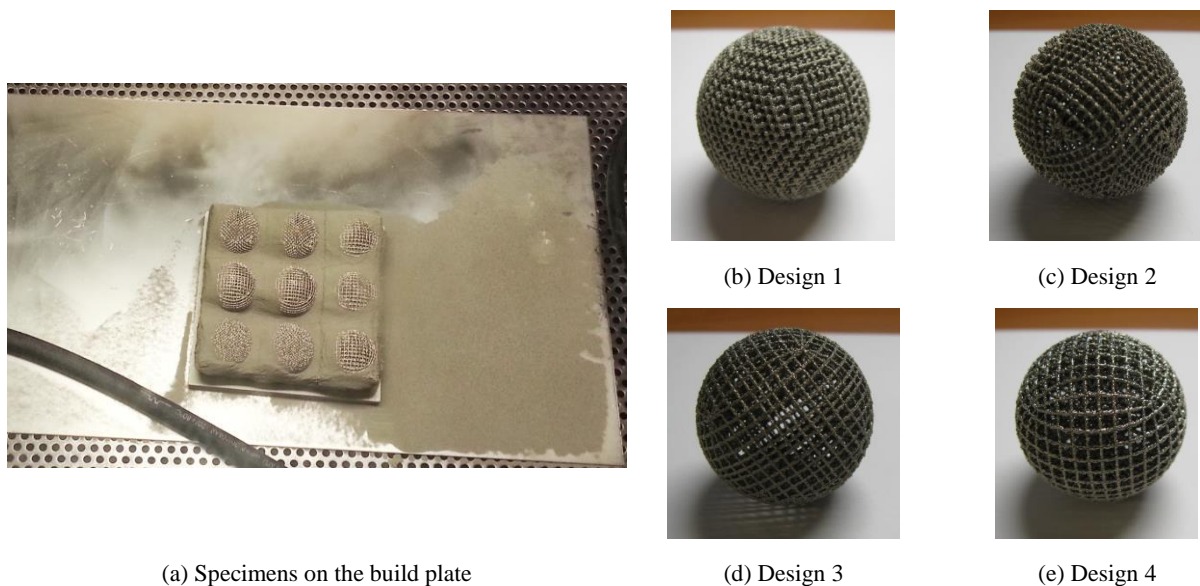


Figure 4 Fabricated meshed balls

Table 2 Comparison of mass

Unit: g	Design 1	Design 2	Design 3	Design 4
Estimated mass in design	9.91	10.09	8.53	8.84
Fabricated mass	28.15	24.7	21.7	26.6
Relative difference (%)	+184%	+145%	+154%	+193%

3 COMPRESSION TEST

To investigate the mechanical properties of mesh balls, we conducted compression tests. The build direction in the EBM machine was used as the axis for the compression tests. Representative force-displacement curves from the compression tests are shown in Figure 5 and the maximum loads and corresponding displacements are listed in Table 3. For comparison purposes, the maximum loads are normalized by mass of meshed balls. Design 4 composed of pentahedral unit cells carried the highest forces that is 147% more than design 1, which was designed by the uniform lattice approach.

There are two noticeable points. The first is that design 1 endured higher force than designs 2 and 3. This means that our first hypothesis cannot be validated by this particular example. Although the conformal lattice approach gives more possibilities to design higher strength lattice structure, the strength of a lattice structure is also governed by details of its geometrical connectivity. The conformal lattice approach insures that lattice structures are fully connected in a layer. However, this does not guarantee that the connectivity is always aligned to a direction of the external load. In case of design 4, since many struts are aligned with the compressive force direction, the measured strength is much higher than other meshed balls.

Next, the force-displacement curve of design 3 indicates that struts in the meshed ball are buckled. This can be observed in the crashed geometry. Since there are no internally connected struts in the cubic unit cell, the buckling mode limits the strength of cubic unit cell lattice structure although the arrangement of struts are parallel to the external force. On the other hand, other meshed balls comprised of diamond and pentahedral unit cells show fracture mode failure.

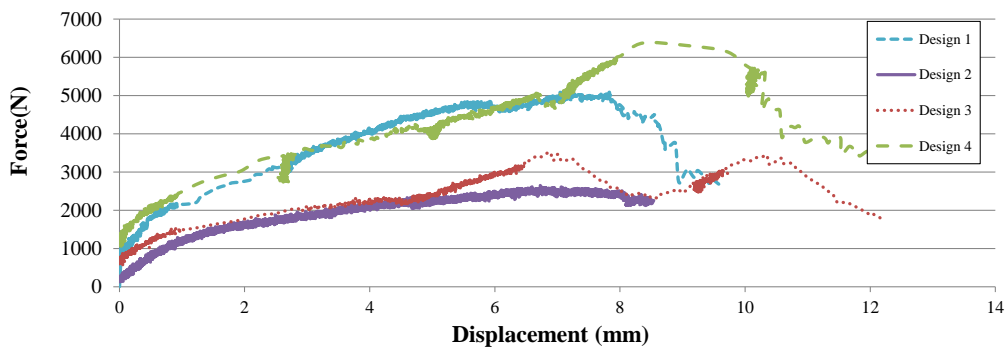


Figure 5 Force-displacement curve during test

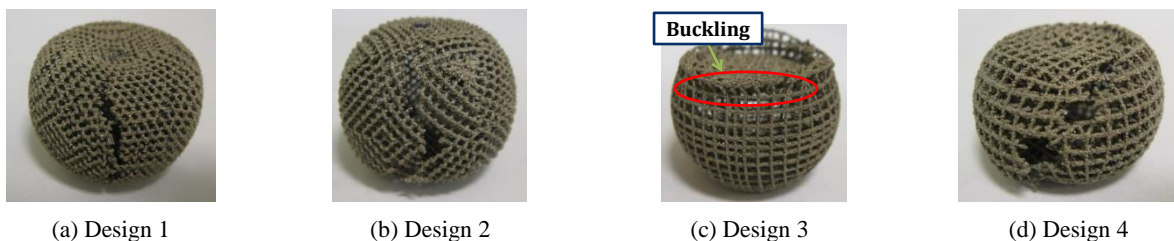


Figure 6 Specimens after compression test

Table 3 ultimate force and corresponding displacement

Design	Ultimate force (N)	Force/Mass (N/g)	Displacement at ultimate force (mm)
1	5034.9	178.86	7.47
2	2554.1	103.40	6.53
3	3512.4	161.86	6.89
4	6844.0	264.59	8.70

4 DETERMINING MASS-EQUIVALENT STRUT DIAMETER

In order to investigate shape variations due to the EBM process, the selected fabricated balls of designs 1 and 4 are observed through the microscope. Figure 7 shows representative strut surfaces from two orientations. When observed in the direction parallel to the build direction, the surfaces are smooth without unmelted powder and stair-steps can be detected based on boundary of the melting pool. However, in the direction perpendicular to building direction, lots of unmelted powder is stuck on strut surfaces. The reason for this phenomenon is that the electron beam melts powder in the top layer of the powder bed and powder particles below the top layer partially melt or otherwise adhere to the melt pool and protrude from the strut surfaces. As a result, the unmelted powder produces shape variations and rough surfaces.

The fabricated strut diameters are measured in digital images taken from a microscope. Table 4 lists minimum, maximum and average value of measured strut diameters. In the case of design 1, the maximum and minimum values are 0.79 mm and 0.452 mm, respectively, while the design strut diameter is 0.4 mm and for design 4 which has a designed diameter of 0.35 mm, the maximum and minimum values are 0.737 mm and 0.377 mm. Based on observation, it is noted that large variations in dimension exist due to the EBM process. Large variations in dimension make it difficult to measure geometrical information such as volume and size of struts.

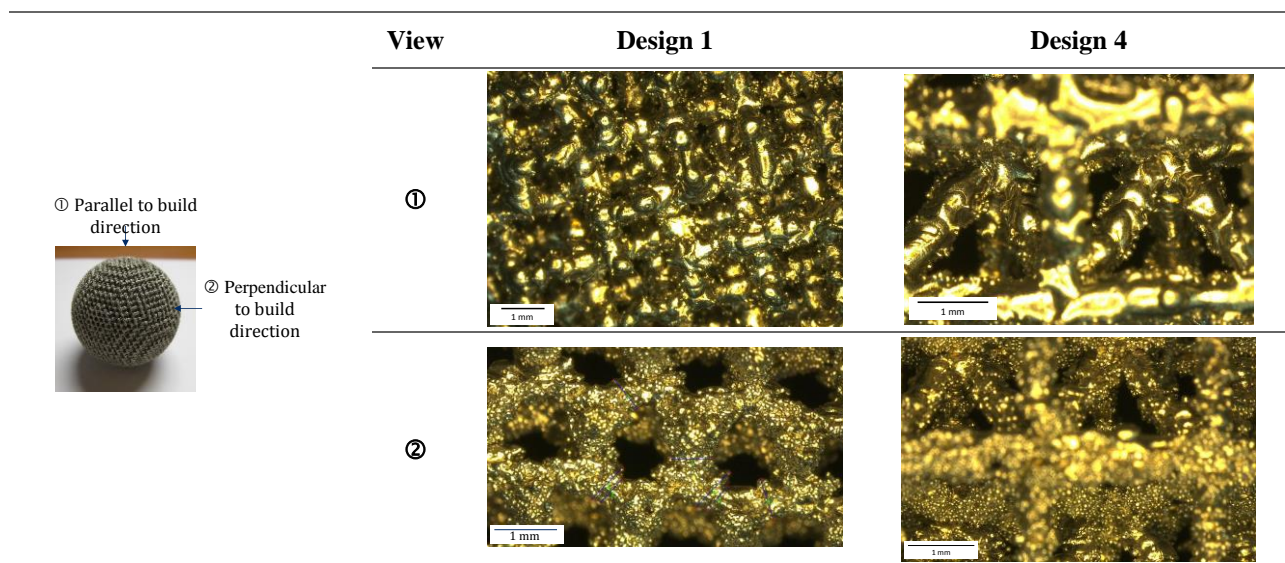


Figure 7 Magnification of fabricated balls

Table 4 Size of fabricated strut

Unit: mm	Designed	Min.	Max.	Average
Design 1	0.4	0.452	0.79	0.610
Design 4	0.35	0.377	0.737	0.546

Table 5 Mass-equivalent strut diameters

	Design strut diameter (mm)	Mass-equivalent strut diameter (mm)	Estimated mass with mass-equivalent strut diameter (g)	Fabricated mass (g)	Relative error
Design 1	0.4	0.725	28.90	28.15	2.66 %
Design 2	0.35	0.650	24.34	24.70	-1.46 %
Design 3	0.4	0.725	21.35	21.70	-1.61 %
Design 4	0.35	0.637	26.61	26.60	0.04 %

The mass-equivalent strut diameter is proposed in order to quantify the effect of shape variations on geometrical dimensions. The mass-equivalent strut diameter is the diameter which gives the same mass in the designed ball as in the fabricated part. To find the mass-equivalent strut diameter, parametric studies were conducted. Meshed ball volumes were calculated in Magics. Based on the strut diameter and corresponding volume of meshed ball design, regression models were generated. The mass-equivalent strut diameters are summarized in Table 5. Compared to designed strut diameters, the mass-equivalent strut diameters are about 1.8 times greater. The estimated masses of meshed balls using the mass-equivalent strut diameters show less than 3% relative error with respect to mass of the fabricated balls. This means that the fabricated dimensions are shifted from the design due to shape variation during the EBM process and the deviations seem to be systematic and repeatable.

5 DETERMINING RESPONSE-EQUIVALENT STRUT DIAMETER

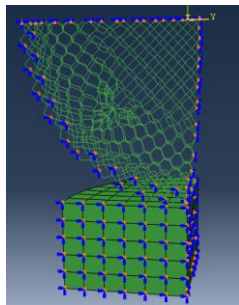
Mass-equivalent strut diameters can be used for measuring mismatch in geometrical aspects such as the mass and volume between a desired lattice and a fabricated lattice. However, fabricated lattice structures cannot support the mechanical load that would be expected from a lattice with the mass-equivalent strut diameter since partially melted powder particles are partially bonded to the strut but do not necessarily contribute to its mechanical properties. Microscopic observations in the previous research show there exist critical defeats in the cross section of struts which degrade the structural performance.[14] In order to quantify the effects of shape variation due to the EBM process on the mechanical response, the response-equivalent strut diameter is introduced and calculated in this section.

To simulate compression test in the previous section, the geometrical information of conformal meshed balls are exported to ABAQUS. Figure 8 (a) shows the finite element analysis (FEA) model of design 2 for finite element analysis. One-eighth model of meshed ball is used and symmetric boundary conditions are applied. Shear flexible beam elements are used to

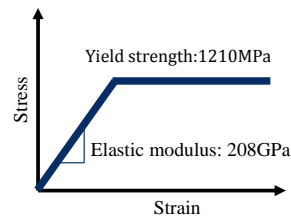
model struts. To describe plastic deformation during compression tests, the plastic constitutive model of Inconel 718 is applied and shown in Figure 8 (b). For elastic deformation, the elastic modulus is set to 208 GPa and 1210 MPa is assigned for the plastic behavior and yield strength. Frictionless contact is assumed at the interface between the meshed ball and the grip. The grip is moved upward as 4mm so that 8mm of the displacement in total is simulated.

To compare the responses of numerical analysis with the test result, the design strut diameters are assigned to each strut in the three meshed balls. Figure 9 describes the force – displacement history of meshed balls. The responses follow the trends of the test but there are large differences in absolute values of forces which the balls support. Table 6 lists ultimate forces during simulations. The ultimate force from FEA is significantly lower than the test results. It is worth noting that the overshoot is observed in case of design 3. This is because in this simulation the buckling phenomenon is not formulated. Therefore, the peak in the design 3 curve near a displacement value of 6 mm of Figure 9 was selected as the ultimate force. The force ratios in Table 6 are ratio between ultimate forces in each ball and that of design 2. The ratios from the analysis are close to those from the compression test.

In order to find the response-equivalent strut diameter a parametric study was performed by re-running the FEA models for different strut diameters. Figure 10 compares four different force-displacement histories of meshed balls with the compression test result for design 4. Based on the parametric study the regression models were constructed to find response-equivalent strut diameters. The response-equivalent strut diameters were calculated using regression models and listed in Table 7. The difference between calculated ultimate forces and compression test results are below 0.5%.



(a) Numerical model of compression test



(b) Material model of Inconel 718

Figure 8 Finite element Analysis model

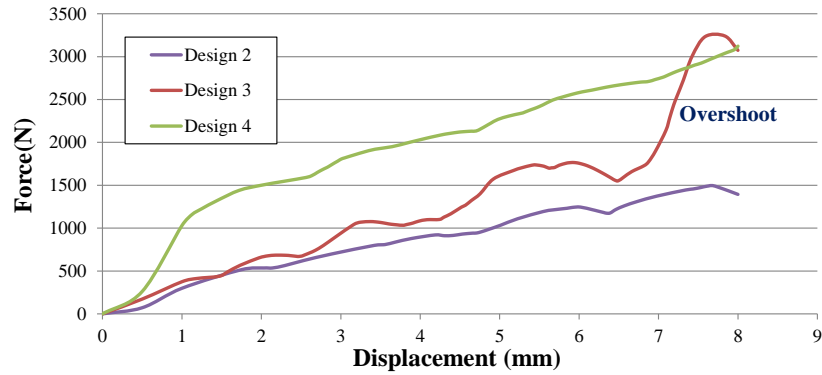


Figure 9 Force-displacement history

Table 6 Comparison of ultimate force

	FEA		Test	
	Ultimate force (N)	Ratio	Ultimate force (N)	Ratio
Design 2	1393.7	1	2554.1	1
Design 3	1765.6	1.27	3512.4	1.38
Design 4	3123.0	2.24	6844.0	2.67

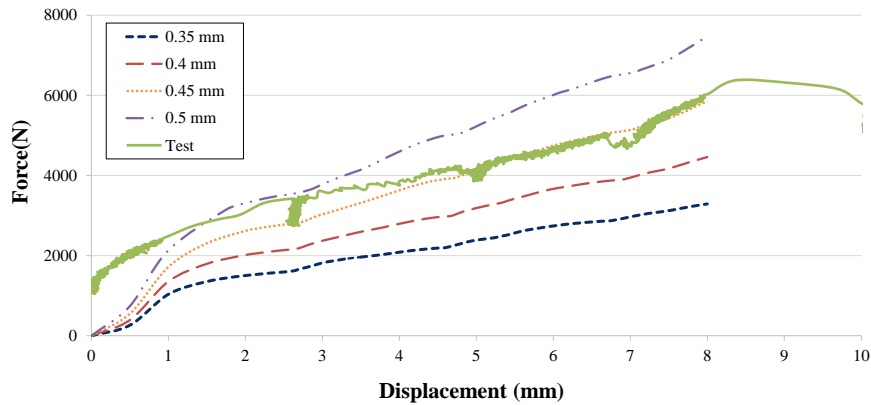


Figure 10 Parametric study for response equivalent diameter of design 4

Table 7 Equivalent strut diameters

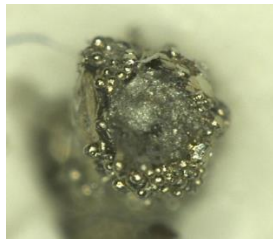
	Design strut diameter (mm)	Mass-equivalent strut diameter (mm)	Response-equivalent strut diameter (mm)	Calculated ultimate force (N)	Compression Test (N)	Relative error
Design 2	0.35	0.650	0.434	2660.6	2649.0	0.44 %
Design 3	0.4	0.725	0.506	3520.2	3512.4	0.22 %
Design 4	0.35	0.637	0.456	6024.9	6041.5	-0.27 %

6 COMPARISON OF MASS-EQUIVALENT AND RESPONSE-EQUIVALENT STRUT DIAMETERS

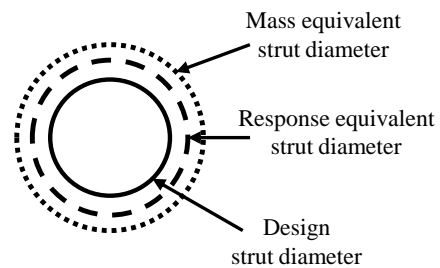
The results from Sections 4 and 5 show that equivalent strut diameters deviate from the design strut diameters and the fabricated lattice structure cannot perform as well as predicted by the mass-equivalent lattice structure. Table 8 shows that mass-equivalent strut diameters are about 1.8 times thicker and response-equivalent strut diameters are about 1.25 times thicker than design strut diameters. The trends of the results correspond well with the cross section of a fabricated strut shown in Figure 11 (a). The fully melted region is shown in the core of the strut and the unmelted powder is stuck on the melting region. The powder contributes to the mechanical performance but the contribution is limited. However, the powder increases the dimensions so that mass-equivalent strut diameters are much larger than design strut diameters. The diameters are compared schematically in Figure 11 (b).

Table 8 Ratios among diameters

	Mass-equivalence to design	Response-equivalence to design
Design 1	1.81	
Design 2	1.86	1.24
Design 3	1.81	1.26
Design 4	1.82	1.28



(a) Cross section of a fabricated strut



(b) Schematic comparison among diameters

Figure 11 Comparison among diameters

7 CONCLUSION

In this paper, several meshed balls were designed and fabricated in order to investigate the effects of design methods and the EBM process on the geometrical and mechanical properties of a lattice structure. The first hypothesis we proposed was not supported since improper selection of unit cells in the conformal lattice approach can weaken the strength of the lattice structure. However, since the conformal lattice approach provides more design possibility such as lattice directions, more durable lattice structures can be designed by the approach, we believe.

Related to the second hypothesis, two equivalent-strut diameters can represent the amount of deviation from designed diameters in geometrical and mechanical aspects. The mass-

equivalent strut diameter can be used for estimation of volume and the size of the struts after fabrication. The response equivalent strut diameters can be utilized in the evaluation process for changes in mechanical behavior of lattice structure due to the EBM process. Future work is to set the functional relationship between equivalent strut diameters and EBM process parameters. The relationship can provide mapping for better fabrication using EBM process.

8 ACKNOWLEDGMENT

Financial support for this work has been funded by National Science Foundation (NSF) grant CMMI-1200788. The authors would like to appreciate Larry Lowe and William Sames at Oak Ridge National Laboratory for fabricating specimens. The authors also would like to thank professor Seung-kyum Choi at Georgia Tech for advising.

9 REFERENCE

1. Ashby, M., *Hybrid Materials to Expand the Boundaries of Material-Property Space*. Journal of the American Ceramic Society, 2011. **94**(s1): p. s3-s14.
2. Evans, A.G., J.W. Hutchinson, N.A. Fleck, M.F. Ashby, and H.N.G. Wadley, *The topological design of multifunctional cellular metals*. Progress in Materials Science, 2001. **46**(3–4): p. 309-327.
3. Deshpande, V.S., N.A. Fleck, and M.F. Ashby, *Effective properties of the octet-truss lattice material*. Journal of the Mechanics and Physics of Solids, 2001. **49**(8): p. 1747-1769.
4. Wang, H.C., Y. and D.W. Rosen, *A hybrid geometric modeling method for large scale conformal cellular structures*, in *ASME Computers and Information in Engineering Conference*. 2005: Long Beach, California.
5. Engelbrecht, S., L. Folgar, D.W. Rosen, G. Schulberger, and J. Williams, *Cellular Structures for Optimal Performance in Solid Freeform Fabrication Symposium*. 2009: Austin, Texas.
6. Wadley, H.N.G., N.A. Fleck, and A.G. Evans, *Fabrication and structural performance of periodic cellular metal sandwich structures*. Composites Science and Technology, 2003. **63**(16): p. 2331-2343.
7. George, T., V.S. Deshpande, K. Sharp, and H.N.G. Wadley, *Hybrid core carbon fiber composite sandwich panels: Fabrication and mechanical response*. Composite Structures, 2014. **108**(0): p. 696-710.
8. Harrysson, O.L.A., O. Cansizoglu, D.J. Marcellin-Little, D.R. Cormier, and H.A. West II, *Direct metal fabrication of titanium implants with tailored materials and mechanical properties using electron beam melting technology*. Materials Science and Engineering: C, 2008. **28**(3): p. 366-373.
9. Marin, E., S. Fusi, M. Pressacco, L. Paussa, and L. Fedrizzi, *Characterization of cellular solids in Ti6Al4V for orthopaedic implant applications: Trabecular titanium*. Journal of the Mechanical Behavior of Biomedical Materials, 2010. **3**(5): p. 373-381.
10. Gibson, I., D.W. Rosen, and B. Stucker, *Additive Manufacturing Technologies: Rapid Prototyping to Direct Digital Manufacturing*. 2010: Springer US.
11. Cansizoglu, O., O. Harrysson, D. Cormier, H. West, and T. Mahale, *Properties of Ti-6Al-4V non-stochastic lattice structures fabricated via electron beam melting*. Materials Science and Engineering: A, 2008. **492**(1–2): p. 468-474.
12. Yang, L., O. Harrysson, H. West II, and D. Cormier. *Design and characterization of orthotropic re-entrant auxetic structures made via EBM using Ti6Al4v and pure copper*. in *International Solid Freeform Fabrication Symposium*. 2011.
13. Parthasarathy, J., B. Starly, S. Raman, and A. Christensen, *Mechanical evaluation of porous titanium (Ti6Al4V) structures with electron beam melting (EBM)*. Journal of the Mechanical Behavior of Biomedical Materials, 2010. **3**(3): p. 249-259.
14. List, F.A., R.R. Dehoff, L.E. Lowe, and W.J. Sames, *Properties of Inconel 625 mesh structures grown by electron beam additive manufacturing*. Materials Science and Engineering: A, 2014. **615**(0): p. 191-197.
15. Nguyen, J., S.-I. Park, D.W. Rosen, L. Folgar, and J. Williams, *Conformal Lattice Structure Design and Fabrication in Solid Freeform Fabrication Symposium*. 2012: Austin, Texas.